Mechanistic Aspects of HC-SCR over HZSM-5: Hydrocarbon Activation and Role of Carbon−Nitrogen Intermediates

Hanna Härelind Ingelsten,*,†,‡ Anders Palmqvist,†,‡ and Magnus Skoglundh†,‡

Competence Centre for Catalysis, and Department of Chemical and Biological Engineering/Applied Surface Chemistry, Chalmers University of Technology, SE-412 96 Göteborg, Sweden

Received: June 13, 2006

This study focuses on the mechanism of lean NO_2 reduction by hydrocarbons (propane, propene, and isobutane) over HZSM-5. In-situ FTIR measurements indicate a close correlation between formation of isocyanate species, consumption of water (formed in the reaction), and formation of amine species. The results in this investigation confirm our previously suggested reaction mechanism, which involves reaction of NO^+ species and hydrocarbon-derived species over Brønsted acid sites, forming isocyanate species. These species are hydrolyzed by water, forming amine species and, finally, N_2. Experiments with $^{18}O_2$ show an enhanced oxidation of propane by oxygen, in the presence of NO_2. This effect can possibly be explained by a type of reaction mechanism where gas-phase and/or loosely bound NO_2 react with the adsorbed hydrocarbon-derived species (i.e., carbenium ion adsorbates and/or alkenes), which then more easily react with oxygen.

1. Introduction

Since the HC−SCR concept first was investigated by Iwamoto et al.[1] and Held et al.,[2] the reaction mechanism has been extensively studied and debated. For zeolite materials, there are several possible reaction pathways suggested in the literature. In general, three main groups can be identified.[3,4] These are catalytic decomposition of NO to nitrogen; oxidation of NO to NO_2, which subsequently is reduced by the hydrocarbon through organic intermediates; and partial oxidation of the hydrocarbon forming oxygen- and/or nitrogen-containing intermediate species, which reduce nitrogen oxides to nitrogen. The mechanism for the HC-SCR reaction over Fe/MFI catalysts has, for instance, been discussed by Chen et al.[5,6] in terms of NO oxidation, and formation of a C-, O-, H-, and N-containing deposit. Yeom et al.[7] propose that nitrogen oxides and organic compounds react and form nitromethane, from which isocyanic acid (HNCO) may be formed via the aci-form of the nitromethane. Ammonia is then suggested to form by hydrolysis of the HNCO with water and then further react with the nitrogen oxides to form ammonium nitrite and finally N_2. The HC-SCR reaction has also been investigated by the reaction of NO with higher nitro paraffins,[8,9] and the mechanism that emerged from these studies involves formation of isocyanate species, likely formed via the aci-form over Brønsted acid sites. The N_2 formation is then suggested to proceed either by hydrolysis of isocyanate with water, forming amine species (and/or ammonia), followed by an SCR reaction, or by a reaction between NO_2 and the deposited isocyanate species. In previous studies,[10−12] we discuss the reaction pathway for lean NO_2 reduction by propane and isobutane over HZSM-5 zeolites. The most important steps involve formation of NO^+ species on the catalytic surface and activation of the hydrocarbon, likely through interaction with the Brønsted acid sites, forming carbenium ion adsorbates and alkenes. These two types of species are proposed to react, forming isocyanate species, which may be hydrolyzed by water, forming amine species that eventually react with other NO^+ species to form N_2.

The activation and oxidation of the hydrocarbon is a prerequisite for the reaction to occur. It has been debated whether NO and/or NO_2 may facilitate the activation of the hydrocarbon and take an active role in the hydrocarbon oxidation. For instance, Petunchi and Hall[13] investigated the lean NO_x reduction by isobutane over Cu-ZSM-5, and they concluded that NO_2 is a stronger oxidizing agent than either NO and oxygen for this system. The gas-phase oxidation of hydrocarbons has also been studied and discussed in terms of NO_2 involvement in the oxidation. Otsuka et al.[14] studied the gas-phase oxidation of a number of saturated hydrocarbons in excess oxygen, with and without NO. They found that the oxidation takes place at lower temperature in the presence of NO and that the activation energy for the conversion of ethane and propane decreases drastically in the presence of NO. They suggested that the reaction is initiated by abstraction of hydrogen by NO_2, forming an alkyl radical.[15] This type of mechanism has also been suggested by Lukyanov and co-workers.[16] It is, thus, certain that NO_2 plays a vital role in the oxidation/activation of the hydrocarbon in the lean NO_x reduction by saturated hydrocarbons.

Previous results show 40% and 55% conversion, respectively, for lean NO_2 reduction by propane and isobutane over the HZSM-5 sample used in the present study.[11,12] In this investigation, we focus on the adsorption and activation of the hydrocarbon in the absence and presence of NO_2 over HZSM-5, which is a prerequisite for NO_x reduction and hydrocarbon oxidation. In particular, we have studied the formation of intermediate CNO species on the catalyst surface and the influence of nitrogen dioxide on the hydrocarbon oxidation using isotope-labeled oxygen.

2. Experimental Methods

The catalyst used in this study was a HZSM-5 zeolite (Akzo Nobel Catalysts BV) with a SiO_2/Al_2O_3 molar ratio of 40.

* Corresponding author. Tel.: +46 31 772 2959. Fax: +46 31 16 00 62. E-mail: hannahi@chalmers.se.

† Competence Centre for Catalysis.

‡ Department of Chemical and Biological Engineering/Applied Surface Chemistry.

10.1021/jp063683z CCC: $33.50
Published on Web 09/01/2006

Textural data, acidic characterization, and preparation of the sample have been reported previously.[11]

In-situ FTIR (Fourier transform infrared) spectroscopy measurements were carried out using a BioRad FTS 6000 spectrometer in diffuse reflection (DRIFT) mode.[17,18] The experimental procedure was previously described in detail.[11] Briefly, the gases, Ar (99.9997%), O_2 (99.95%), NO_2 (5000 ppm in Ar), C_3H_8 (10% in Ar), C_3H_6 (4% in Ar), and *i*-C_4H_{10} (2% in Ar), were introduced via separate mass flow controllers (Bronkhorst Hi-Tech) to the DRIFT cell. The sample was initially pretreated in nitrogen dioxide and oxygen (1000 ppm NO_2 and 10% O_2, balanced with Ar, 500 °C, 40 min) followed by oxygen (10% O_2 in Ar, 500 °C, 1 h) and then evacuated in pure Ar (500 °C, 15−60 min) at a total flow rate of 300 mL/min. Background spectra (50 scans at a resolution of 1 cm^{-1}) were collected under Ar exposure. Fresh samples were used for all experiments.

The reaction between hydrocarbon, oxygen, and nitrogen dioxide was studied by DRIFT experiments. The sample was exposed to hydrocarbon (800 ppm propane, 800 ppm propene, or 200 ppm isobutane) with and without oxygen (10%), and spectra were recorded until steady-state conditions were reached at 450, 400, and 350 °C, respectively. Subsequently 1000 ppm NO_2 was introduced (in excess oxygen), and three spectra per second were taken during the first minutes of exposure, and then spectra were taken every 5 min until steady-state.

The influence of NO_2 on the propane oxidation was investigated with isotope-labeled oxygen ($^{18}O_2$) at 350 and 450 °C (the pretreatment was performed with $^{18}O_2$). In sequence 1, the sample was exposed to propane (2000 ppm) and $^{18}O_2$ (1.5%) during 1 h. In the second sequence, NO_2 (1000 ppm) was introduced to the sample cell, and finally, in sequence 3, $^{16}O_2$ was introduced and the $^{18}O_2$ supply was turned off. The experiments were monitored by DRIFT spectroscopy and the gas composition after the sample was probed using a quartz capillary and continuously measured by a quadrupole mass spectrometer (Balzers QMS 200). The analyzed *m*/*e* ratios were: 28 ($C^{16}O$, $C^{16}O_2$, $C^{16}O^{18}O$, N_2), 29 (C_3H_8), 30 ($C^{18}O$, $C^{18}O_2$, $C^{16}O^{18}O$, $N^{16}O$, $N^{16}O_2$), 32 ($^{16}O_2$), 34 ($^{16}O^{18}O$), 36 ($^{18}O_2$), 40 (Ar), 44 ($C^{16}O_2$, $N_2{}^{16}O$), 46 ($C^{16}O^{18}O$, $N^{16}O_2$), and 48 ($C^{18}O_2$). In addition, $N^{18}O$, $N^{18}O^{16}O$, and $N^{18}O_2$ may contribute to *m*/*e* 32, $N_2{}^{18}O$ to *m*/*e* 46, and $N^{16}O^{18}O$ to *m*/*e* 48. It seems, however, less likely that any significant amounts of these species were formed.

3. Results and Discussion

The FTIR measurements are mainly presented for the region above 2000 cm^{-1} because below 2000 cm^{-1} the background noise level is significant, probably related to perturbed vibrations of the zeolite framework,[19−21] which makes peak observation and assignment difficult in this range.

3.1. Formation of Adsorbed Surface Species during the Reduction of NO_2 with Hydrocarbons in Lean Environment. The formation of adsorbed surface species is followed in-situ by DRIFT spectroscopy directly after a change in gas composition is made and NO_2 is introduced to a gas stream containing hydrocarbon and excess oxygen. Propane is used as the main model hydrocarbon in this study, but for comparison also propene and isobutane have been investigated with emphasis on observed differences as compared to propane.

3.1.1. Exposure to Hydrocarbon and Oxygen. When propane is introduced to the HZSM-5 sample, one peak centered around 2968 cm^{-1} develops (Figure 1a), which is assigned to C−H vibrations from propane in the gas phase and/or weakly bound to the sample surface.[22−24] The double peak around 2360 cm^{-1}

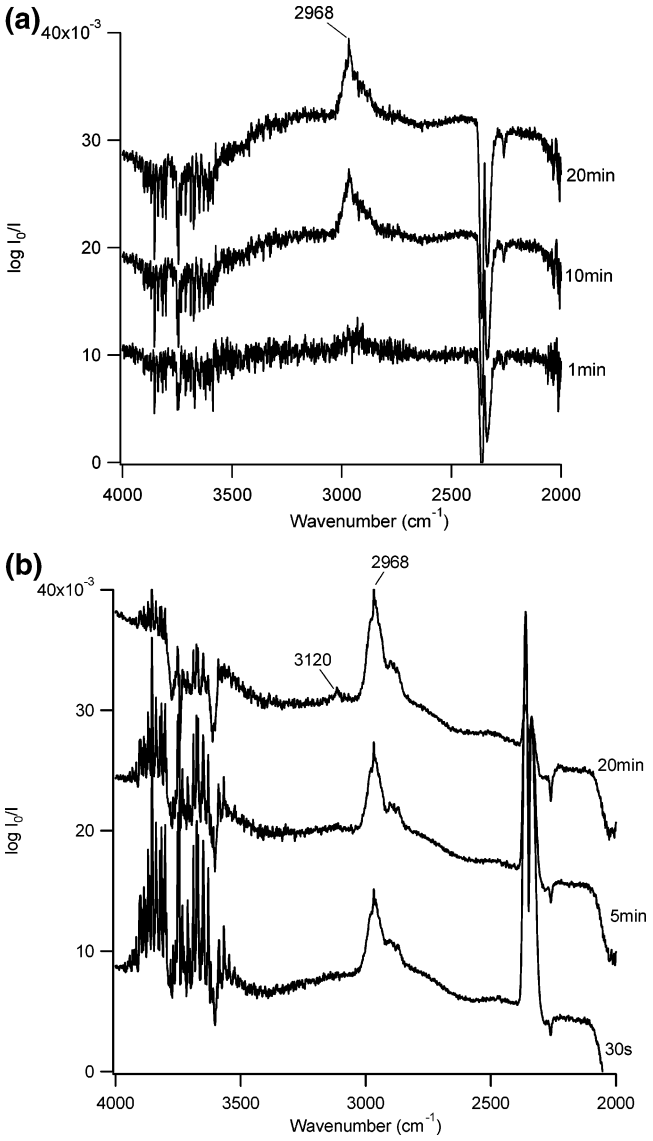

Figure 1. (a) Adsorption of propane (C_3H_8) over HZSM-5, followed by DRIFT spectroscopy at 450 °C. (b) Adsorption of propane (C_3H_8) and O_2 over HZSM-5, followed by DRIFT spectroscopy at 450 °C.

(Figure 1a and b) is attributed to CO_2 in the gas phase, likely due to changes in the background. Figure 1b shows the evolution of peaks when oxygen is added to the inlet gas stream at 450 °C. Apart from the propane peak, which is constant, a peak appears around 3120 cm^{-1} after about 15 min of exposure to propane and oxygen at 450 °C, which likely is due to C−H vibrations from unsaturated hydrocarbons.[6,22] This peak is not observed at lower temperatures. Negative absorption peaks arise (after ca. 15 min) at 3745 and 3610 cm^{-1}, which are assigned to O−H stretching vibrations originating from silanol groups (Si−OH) and Si(OH)Al bridging hydroxyl groups (Brønsted acid sites), respectively.[20,21,24−29] Because the time scale is similar for the appearance of the 3120 cm^{-1} peak and the Brønsted peak, it is probable that the propane interacts with the Brønsted acid sites, forming carbenium ion adsorbates[30] and eventually alkenes.

For comparison, propene (Figure 2a) and isobutane (Figure 2b) have also been adsorbed on the sample. Both hydrocarbons show peaks in the C−H stretching region (2800−3000 cm^{-1}).[22−24] In addition, a peak appears around 3130 cm^{-1} for propene, likely due to C−H stretching vibrations from unsaturated hydrocarbons.[6,22] A broad peak, centered around 2450 cm^{-1}, is visible

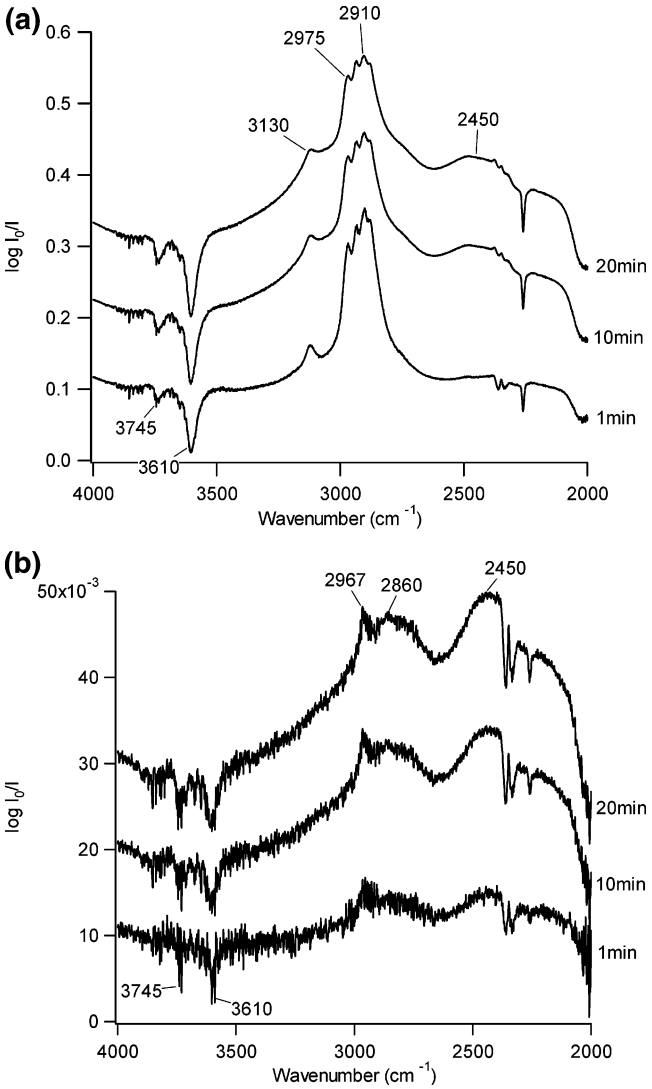

Figure 2. (a) Adsorption of propene (C_3H_6) over HZSM-5, followed by DRIFT spectroscopy at 400 °C. (b) Adsorption of isobutane (C_4H_{10}) over HZSM-5, followed by DRIFT spectroscopy at 350 °C.

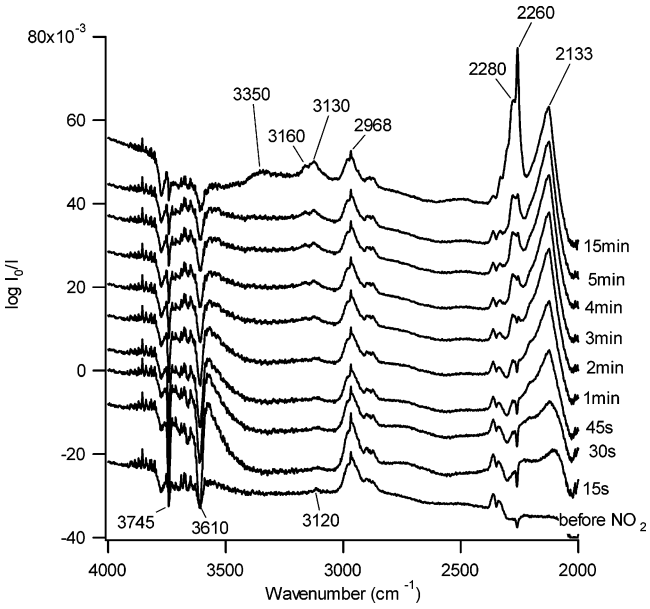

Figure 3. Introduction of NO_2 to the reaction gas mixture (propane + O_2) over HZSM-5, followed by DRIFT spectroscopy at 450 °C.

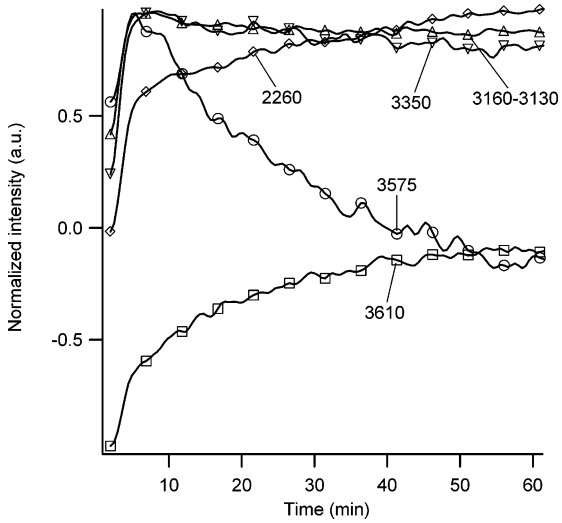

Figure 4. Evolution of functional groups during introduction of NO_2 to the reaction gas mixture (propane + O_2) over HZSM-5, followed by DRIFT spectroscopy at 450 °C.

for both propene and isobutane, which can be assigned to O−H stretching vibrations of water, hydrogen bonded to Lewis acid sites in the HZSM-5 framework.[20] The peak attributed to Brønsted acid sites appears immediately for propene, while for isobutane this peak develops during the first minutes of exposure to the hydrocarbon. When oxygen is introduced, the peak development is similar to the propane case.

3.1.2. Addition of NO_2 to the Reaction Gas Mixture. Upon introduction of NO_2 to the reaction gas mixture, several peaks appear in the DRIFT spectra as shown in Figures 3−5. The assignments of these are summarized in Table 1. The evolution of peaks is most easy to follow for the propane case; however, peaks in the same regions appear for all three hydrocarbons. At steady-state conditions in the presence of hydrocarbon, O_2, and NO_2, well-established peaks are found at 2133, 2260 with a shoulder at 2280, and a double peak around 3130 and 3160 cm^{-1}. The first peak (2133 cm^{-1}) is assigned to nitrosonium ions (NO^+),[25] and the peak at 2260 cm^{-1} with the shoulder at 2280 cm^{-1} is most likely attributed to isocyanate (−NCO) species bound to Al and Si in the zeolite framework, respectively,[6,22,24,31−36] and/or to nitrile species.[5,6,22,24,31] For the saturated hydrocarbons (propane and isobutane), the small peak around 3130 cm^{-1} grows, and a second peak around 3160 cm^{-1} appears when NO_2 is introduced. For the propene case, the single peak at 3140 cm^{-1} grows upon introduction of NO_2. These peaks are likely attributed to C−H vibrations from unsaturated hydrocarbons when only oxygen and hydrocarbon are present, as postulated previously. However, when NO_2 is introduced to the sample cell (together with oxygen and hydrocarbon), these peaks can possibly arise from N−H vibrations in amine species, which has also been suggested in the literature.[6,37,38] An additional explanation might, however, be that unsaturated hydrocarbons are formed in cracking reactions over the Brønsted acid sites[30] and that NO_2 facilitates these reactions. In the N−H stretching region (3200−3400 cm^{-1})[6,22,24,39,40] of Figures 3 and 5, some weak peaks appear around 3350 cm^{-1}, which probably are due to amine species.[37,41,42] No changes are observed in the C−H stretching region (2800−3000 cm^{-1}). For the isobutane and propene cases, the magnitude of the negative O−H peaks (at 3610 and 3745 cm^{-1}) increases when NO_2 is introduced (Figure 5), indicating that species such as hydrocarbons, amine species, and/or water block these sites. For the propane case, however, the Brønsted acid sites partly recover; that is, they are either recreated or the adsorbed species removed (Figures

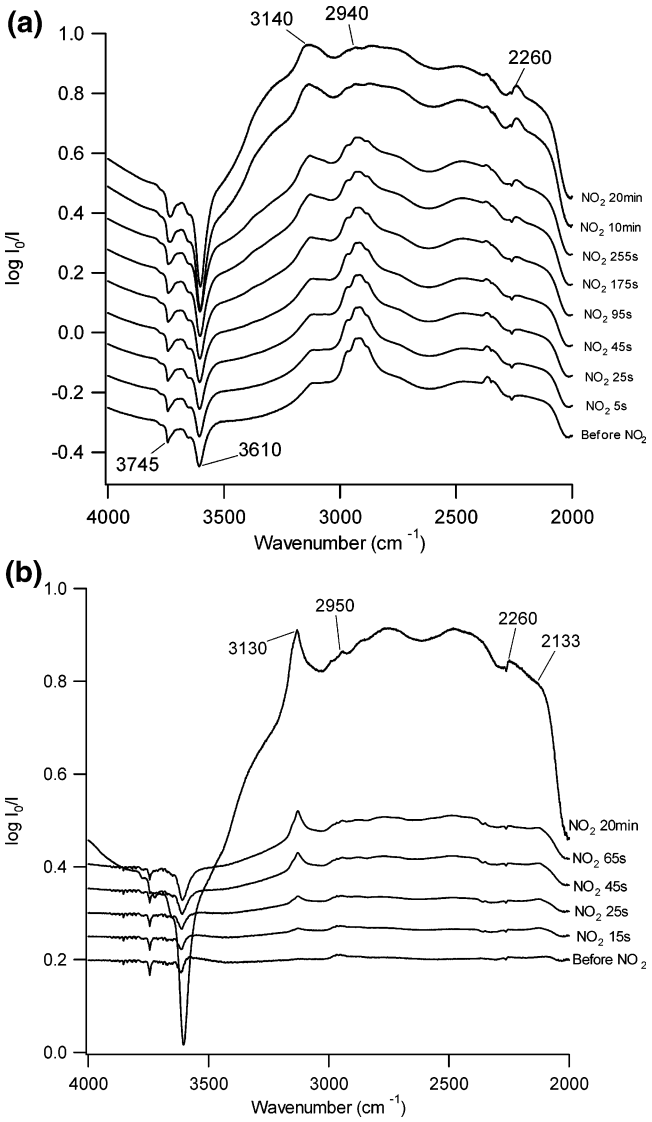

Figure 5. (a) Introduction of NO_2 to the reaction gas mixture (propene + O_2) over HZSM-5, followed by DRIFT spectroscopy at 400 °C. (b) Introduction of NO_2 to the reaction gas mixture (isobutane + O_2) over HZSM-5, followed by DRIFT spectroscopy at 350 °C.

3 and 4). Unlike propane, propene and isobutane are easily activated on acid sites (as was clearly shown in the previous section); thus the conversion of these hydrocarbons is higher, as was previously shown for isobutane,[12] yielding more water, which takes part in the hydrolysis of isocyanate species, forming amine species. These reactions occur most likely on the Brønsted acid sites, and hence these sites become increasingly blocked.

The relative changes in normalized intensity of the different peaks in Figure 3 upon introduction of NO_2 are shown in Figure 4. Initially, water is produced in the reaction, manifested by an increase in the intensity of the O−H vibration peak at 3575 cm^{-1}.[43] During the following period, water is consumed, while at the same time the intensities of the peaks attributed to Brønsted acid sites, adsorbed isocyanate species and nitrosonium ions, increase. Also, the amount of unsaturated hydrocarbons and the amine species increase during this period. It is thus likely that most of the water formed restores the Brønsted acid sites while a fraction is either directly or indirectly involved in the formation of amine species. The intensity of the isocyanate peak increases during the entire experiment, rapidly at start and more moderately after about 10 min, implying that the number of available sites for NCO decreases and that the consumption of NCO species for formation of amines is slower than the NCO formation. The Brønsted peak is intense at start (largely negative as is shown in Figure 3), indicating blocking of these sites, probably by water, isocyanate, and/or amine species. However, with time the Brønsted sites partly recover. The peaks attributed to amine species (around 3350 and 3130−3160 cm^{-1}) and/or unsaturated hydrocarbons (3130−3160 cm^{-1}) increase rapidly after NO_2 is introduced to the sample, reach a maximum, decrease slightly, and arrive at a constant level. Because the evolution of these peaks is very similar, it is likely that also the peaks around 3130−3160 cm^{-1} can be assigned to N−H stretching vibrations (when both NO_2 and hydrocarbon are present). The maximum intensity for these species coincides with the maximum for the water peak and the negative maximum for the Brønsted peak. Hence, it seems reasonable that amine species are formed in the hydrolysis reaction with water and NCO species and that the reaction proceeds over Brønsted acid sites, because these sites initially are blocked. The results presented above support and further emphasize our previously suggested reaction mechanism for this system.[10,11]

Below 2000 cm^{-1} some peaks are found (Figure 6), even though the influence from the zeolite framework[19−21] may be significant in this region. When propane, oxygen, and NO_2 are introduced to the sample, peaks develop at 1730, 1630−1560, and 1310 cm^{-1}. The first peak can probably be assigned to asymmetric stretching vibrations of NO_2 originating from N_2O_4, which possibly forms during adsorption of NO_2 in HZSM-5.[26,31] The two other peaks may be due to asymmetric and symmetric stretching vibrations of NO_2,[26,31] weakly bound to the surface. These peaks (1630−1560 and 1310 cm^{-1}) may also arise from formation of N_2O_3 (O═N−NO_2) on the sample surface; however, the peak attributed to N═O (1930−1880 cm^{-1})[31,44] is only observed during the first minute of NO_2 addition, which render this explanation less probable. Alternatively, the bands at 1630−1560 and 1310 cm^{-1} may be attributed to surface-bound nitrates (NO_3^-) and nitrites (NO_2^-). However, these species are preferably formed on basic oxides, and the NO_2 storage on acidic samples is found to be small or negligible over 300 °C;[45] hence, this is less likely to occur. It is thus probable that NO_2 is adsorbed on the sample surface either as NO_2 or as N_2O_4 and then transforms into NO^+ species, which, according to Hadjiivanov,[25] is the most stable NO species in HZSM-5. In this region (1650−1300 cm^{-1}), the influence from carboxylate and carbonate species formed on the sample surface may also be significant.[46]

3.2. Influence of NO_2 on the Oxidation of Propane. The influence of NO_2 on the oxidation of propane was studied with step-response experiments monitored in-situ by DRIFT spectroscopy combined with mass spectrometer analysis of reactor exhaust composition and using isotope-labeled oxygen.

3.2.1. Effluent Gas Composition. Figures 7 and 8 show the effluent gas composition from the reactions between propane, oxygen, and NO_2 over HZSM-5 at 450 and 350 °C, respectively. Initially, when the sample is exposed to $^{18}O_2$ and propane (sequence 1), formation of species with *m*/*e* 28, 30, 44, 46, and 48 is observed. Because the sample has not been exposed to NO_2 (in this sequence), the formed species are related to $C^{16}O$, and, to a minor extent, to $C^{16}O_2$ and $C^{16}O^{18}O$ (28), $C^{18}O$, and, to a minor extent, to $C^{18}O_2$ and $C^{16}O^{18}O$ (30), $C^{16}O_2$ (44), $C^{16}O^{18}O$ (46), and $C^{18}O_2$ (48). At 450 °C, the formation of $C^{18}O$, $C^{16}O^{18}O$, and $C^{18}O_2$ is clear, while at 350 °C mainly $C^{18}O$ seems to be formed to a significant extent. The peaks observed at the beginning of sequence 1 (at both temperatures) for *m*/*e* 28, 29, and 44 are likely due to adsorption/desorption of propane and

TABLE 1: Summation of the Peak Assignments Made in This Investigation

peak position (cm^{-1})	gas condition[a]	assignment	ref
2133	$NO_2 + O_2$	N−O stretch from NO^+ species	25
2260	$HC + NO_2 + O_2$	−N═C═O stretch (on alumina)	6,22,24,31−36
2280	$C_3H_8 + NO_2 + O_2$	−N═C═O stretch (on silica)	6,22,24,31−36
2325	$C_3H_8 + {}^{18}O_2$	C−O stretch from CO_2 (g) with ^{18}O	48
2340	$C_3H_8 + {}^{18}O_2$	C−O stretch from CO_2 (g) with ^{18}O	48
2360	$HC + O_2$	C−O stretch from CO_2 (g)	48
2450	$C_3H_6 + O_2$ i-$C_4H_{10} + O_2$	O−H stretch from water	20
2800−3000	HC	C−H stretch from saturated hydrocarbons	22−24
2968	C_3H_8	C−H stretch from C_3H_8 (g) and/or loosely bound	22−24
3120, 3130	C_3H_6 $C_3H_8 + O_2$ i-$C_4H_{10} + O_2$	C−H stretch from unsaturated hydrocarbons	6,22
3130, 3140, 3160	$HC + O_2 + NO_2$	C−H stretch from unsaturated hydrocarbons and/or N−H stretch from amine species	6,37,38
3350	$HC + O_2 + NO_2$	N−H stretch from amine species	37,41,42
3575	$C_3H_8 + NO_2 + O_2$	O−H stretch	43
3610	C_3H_6 $C_3H_8 + O_2$ i-C_4H_{10}	O−H stretching vibrations from Si(OH)Al bridging hydroxyl groups	20,21,24−29
3745	C_3H_6 $C_3H_8 + O_2$ i-C_4H_{10}	O−H stretching vibrations from Si−OH	20,21,24−29

[a] All conditions that, at least, include these species.

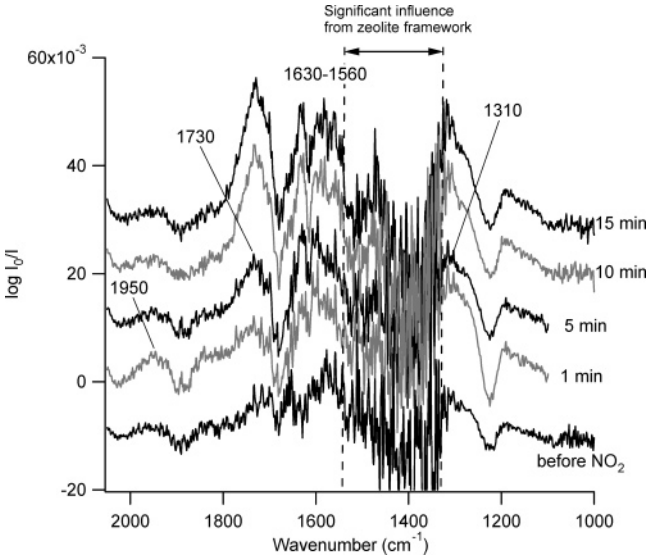

Figure 6. Introduction of NO_2 to the reaction gas mixture (propane + O_2) over HZSM-5, followed by DRIFT spectroscopy at 450 °C, below 2000 cm^{-1}.

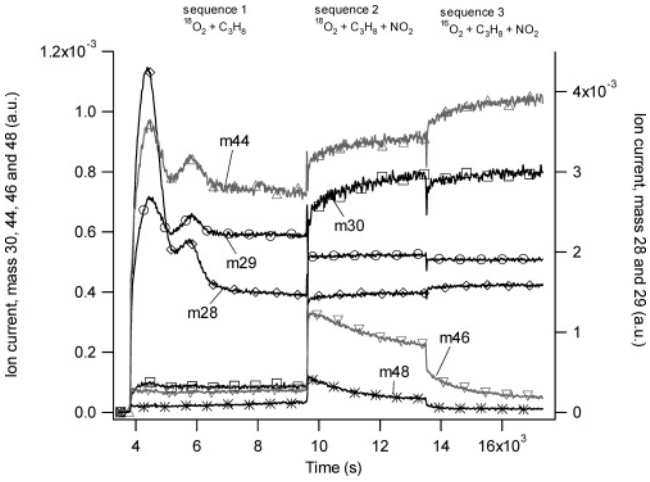

Figure 7. Effluent gases measured by mass spectrometry after reaction of $^{18}O_2$ and C_3H_8 (sequence 1), $^{18}O_2$, C_3H_8, and NO_2 (sequence 2), and $^{16}O_2$, C_3H_8, and NO_2 (sequence 3) over HZSM-5 at 450 °C. Gas composition: 1000 ppm NO_2, 2000 ppm C_3H_8, and 1.5% O_2.

reaction of adsorbed propane with adsorbed oxygen ($^{16}O_2$), forming $C^{16}O$ and $C^{16}O_2$. Even though a thorough pretreatment with $^{18}O_2$, followed by evacuation in Ar, was performed before the experiment started, it is rather unlikely that ^{16}O in the zeolite structure has been exchanged with ^{18}O to a large extent, and hence the initial reaction between adsorbed species results mainly in formation of $C^{16}O$ and $C^{16}O_2$.

At 450 °C (Figure 7), introduction of NO_2 (sequence 2) results in increased signals for *m*/*e* 30, 44, 46, and 48. The propane signal (*m*/*e* 29) decreases, indicating a higher conversion of propane in this sequence, and *m*/*e* 28 is unchanged. The increase in *m*/*e* 30 and 46 is likely attributed to NO and NO_2; however, comparing sequence 2 and 3 indicates that the increase in *m*/*e* 46 (in sequence 2) can not only be attributed to NO_2 but is most likely also due to formation of $C^{16}O^{18}O$. This together with the increase in *m*/*e* 44 implies that oxygen from NO_2 is active in the propane oxidation at 450 °C. Nitrous oxide (N_2O) may also contribute to *m*/*e* 44; however, as was shown previously,[11] the formation of N_2O is low or negligible for this system under these conditions. The increase of $C^{18}O_2$ (*m*/*e* 48), when NO_2 is introduced to the sample, is interesting because this suggests an increased reaction between propane and $^{18}O_2$ when NO_2 is present. It is thus reasonable that NO_2 facilitates the propane oxidation with oxygen, possibly initiating the

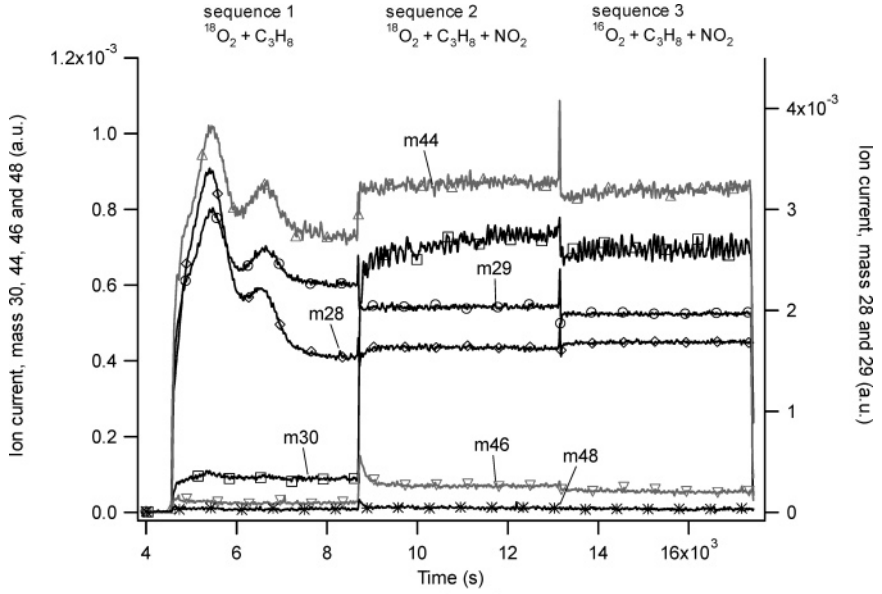

Figure 8. Effluent gases measured by mass spectrometry after reaction of $^{18}O_2$ and C_3H_8 (sequence 1), $^{18}O_2$, C_3H_8, and NO_2 (sequence 2), and $^{16}O_2$, C_3H_8, and NO_2 (sequence 3) over HZSM-5 at 350 °C. Gas composition: 1000 ppm NO_2, 2000 ppm C_3H_8, and 1.5% O_2.

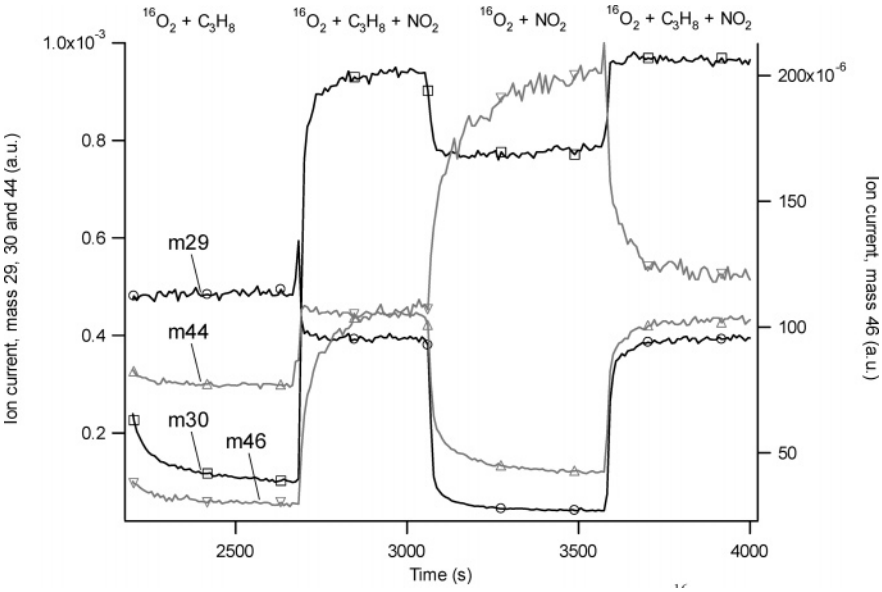

Figure 9. Effluent gases measured by mass spectrometry after reaction of $^{16}O_2 + C_3H_8$; $^{16}O_2 + C_3H_8 + NO_2$; $^{16}O_2 + NO_2$; and $^{16}O_2 + C_3H_8 + NO_2$ over HZSM-5 at 450 °C. Gas composition: 1000 ppm NO_2, 300 ppm C_3H_8, and 10% O_2.

reaction with the hydrocarbon, which then more easily will react with oxygen. Switching the labeled oxygen to $^{16}O_2$ (sequence 3) results, as expected, in an increased formation of $C^{16}O_2$ (*m*/*e* 44) and a decrease in the signals for *m*/*e* 46 and 48, and eventually *m*/*e* 46 reflects only NO_2 in this sequence.

At 350 °C (Figure 8), introducing NO_2 (in sequence 2) results in a decrease in the propane signal and an increase in *m*/*e* 30, 44, and 46, leaving the other signals rather unchanged. The increase in the 44 signal indicates that NO_2 is active in the propane oxidation also at this temperature. However, *m*/*e* 30 and 46 likely mainly reflect NO and NO_2 because the change in these signals is small or negligible, going from sequence 2 to 3. There are no observable changes in *m*/*e* 48 ($C^{18}O_2$), and thus the NO_2 will probably not contribute to activating the hydrocarbon for oxidation with oxygen at this temperature.

For comparison, the same type of experiments was performed with $^{16}O_2$ as sole oxygen source (at 450 °C). The results are shown in Figure 9, and the most interesting feature is the relative change in *m*/*e* 30 (NO) and *m*/*e* 46 (NO_2). Switching the propane supply on (i.e., C_3H_8, O_2, and NO_2 in the inlet gas) results in a decrease in *m*/*e* 46 while *m*/*e* 30 is increasing. This implies that one oxygen atom from the NO_2 molecule is used in the oxidation process of propane, resulting in a net production of NO when propane is present in the inlet gas. Furthermore, *m*/*e* 44 (CO_2) increases both when propane is added to an inlet gas containing oxygen and NO_2, and when NO_2 is added to an inlet gas containing oxygen and propane, indicating an increased oxidation of propane when NO_2 is present in the feed. Hence, these results further support the results from the isotope experiments presented above.

As has been shown previously, the maximum activity for NO_2 reduction by propane over this HZSM-5 sample is reached around 450 °C.[11,12] This is also the temperature range where the promoting effect of NO_2 for oxidation of propane with oxygen becomes important. The propane is likely activated over Brønsted acid sites, as postulated previously,[11,12,18] by accepting a proton, forming alkanium ions, which subsequently rearrange to carbenium ions and eventually alkenes.[30] The enhancement

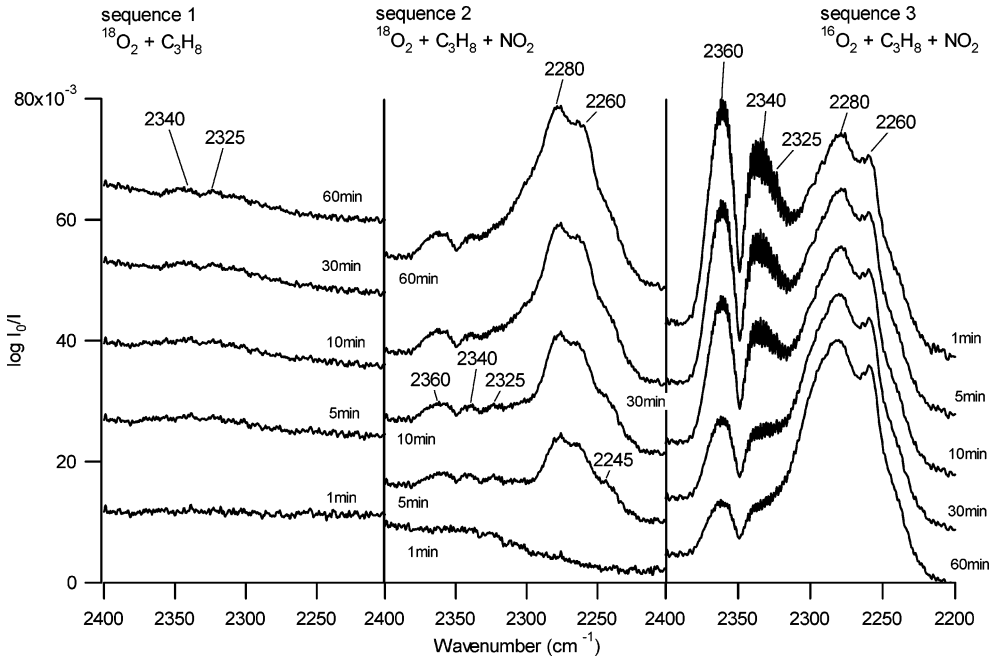

Figure 10. The reaction of $^{18}O_2$ and C_3H_8 (sequence 1), $^{18}O_2$, C_3H_8, and NO_2 (sequence 2), and $^{16}O_2$, C_3H_8, and NO_2 (sequence 3) over HZSM-5, followed by DRIFT spectroscopy at 450 °C.

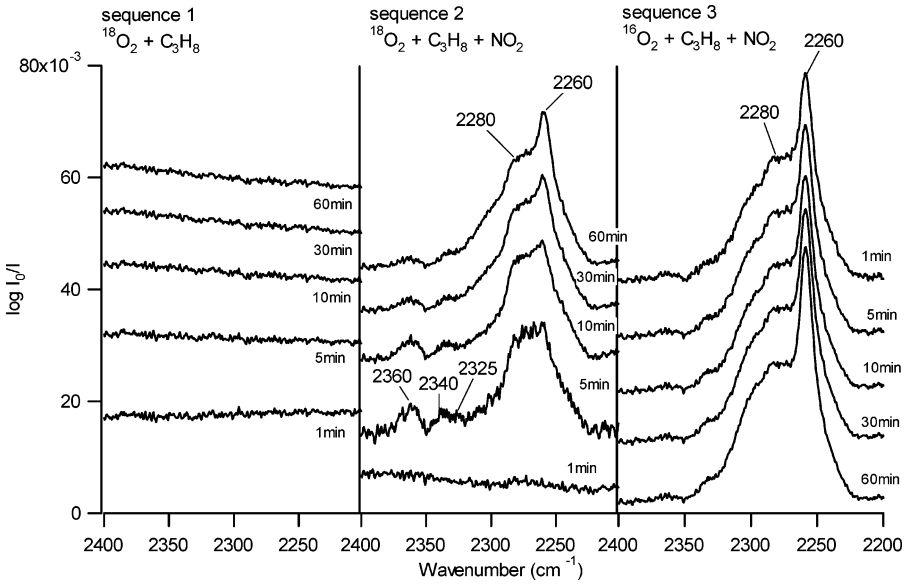

Figure 11. The reaction of $^{18}O_2$ and C_3H_8 (sequence 1), $^{18}O_2$, C_3H_8, and NO_2 (sequence 2), and $^{16}O_2$, C_3H_8, and NO_2 (sequence 3) over HZSM-5, followed by DRIFT spectroscopy at 350 °C.

of propane oxidation, seen when NO_2 is introduced to the reaction gas mixture, can possibly arise from a type of reaction mechanism where an oxygen atom from gas-phase NO_2 and/or loosely bound NO_2 reacts with the adsorbed propane-derived species (i.e., carbenium ion adsorbates and/or alkenes), which then more easily will react with O_2. Considering the zeolite framework, with pore diameters of 5−6 Å,[47] it is not easy to distinguish between NO_2 in the gas phase and NO_2 weakly adsorbed in the zeolite structure. As mentioned in a previous section, DRIFT data show peaks, which may be attributed to weakly bound NO_2. Thus, nitrogen dioxide might be present in the zeolite pore structure as physisorbed species or in the gas phase.

3.2.2. Adsorbed Surface Species. The DRIFT results from the isotope experiments are presented in Figures 10 and 11, focusing on the 2400−2200 cm^{-1} region, where oxygen-containing species such as CO_2 and isocyanate species may be found. In the first sequence with $^{18}O_2$ and propane, some minor peaks are found at 2340 and 2325 cm^{-1} (at 450 °C). Upon introduction of NO_2 (sequence 2), these peaks grow and become visible also at 350 °C. An additional peak at 2360 cm^{-1} is also seen (for both temperatures) when NO_2 is present in the feed gas. These three peaks can most likely be attributed to a combination of different oxygen-isotope CO_2 molecules in the gas phase and/or adsorbed on the sample surface. According to Liao et al.,[48] gas-phase and adsorbed $C^{16}O_2$ give peaks at 2361 and 2349 cm^{-1}, respectively. The corresponding wavenumbers for $C^{16}O^{18}O$ and $C^{18}O_2$ are supposed to be 2350, 2338 and 2343, 2331 cm^{-1}, respectively.[48] When $^{18}O_2$ is exchanged with $^{16}O_2$ (sequence 3), the peaks around 2340 and 2325 cm^{-1} decrease (Figure 10), which further support this assignment. These results are in accordance with the findings from the effluent gas analysis, where the formation of carbon dioxide with 18-oxygen increased when NO_2 was introduced to the reaction gas mixture.

Addition of NO_2 (sequence 2) also results in the development of peaks at 2280 and 2260 cm^{-1} (for both temperatures), and a weaker peak at 2245 cm^{-1} (for 450 °C) (Figures 10 and 11). The two first peaks are likely due to isocyanate (−NCO) and/or nitrile species (as discussed in the previous section). The latter one (2245 cm^{-1}) could probably be attributed to $NC^{18}O$ species, because isotopic exchange with heavier atoms undertakes a red-shift, thus indicating that the O-atom in the isocyanate species may originate, at least to some extent, from O_2 (at 450 °C). A conspicuous result is the relative intensity of the peaks at 2280 and 2260 cm^{-1}. At 450 °C, the 2280 cm^{-1} peak is more intense than the peak at 2260 cm^{-1} (Figure 10), and at 350 °C, the relative intensity of these peaks is the opposite (Figure 11). In previous studies,[10,11] as well as the experiments with unlabeled oxygen presented in this paper, the 2260 cm^{-1} peak is the more intense one of the two peaks (also at 450 °C). The 2280 cm^{-1} peak could be due to overlap with the different CO_2 peaks (at 450 °C), but because the relative intensities of the peaks are sustained in sequence 3, where the isotope-CO_2 peaks decrease and disappear, this explanation seems less likely. However, upon close inspection of Figure 3 (previous section), where the HZSM-5 sample is exposed to propane, $^{16}O_2$, and NO_2, a small shoulder can be observed around 2305 cm^{-1}. According to Solymosi et al.,[49] this peak can be due to asymmetric stretching of NCO species attached to silica. Wichterlová et al.[50] attribute a band around 2300 cm^{-1} to stretching vibrations of CN species bound to bridging OH groups in high silica zeolites. If some of the oxygen, in the NCO species and/or in the OH groups, arises from $^{18}O_2$, it is possible that the peak around 2305 cm^{-1} shifts and hence overlaps with the 2280 cm^{-1} peak. Because it is probable that most of the oxygen in the NCO species originate from NO_2, the peaks at 2260 and 2280 cm^{-1} will still remain. Thus, formation of intermediate carbon−nitrogen species with 18-oxygen may give rise to the observed change in the relative intensities of the two peaks (2260 and 2280 cm^{-1}) at 450 °C. Previous results[10,11] show an accumulation of this kind of species on the sample surface during the reaction, which may explain why the relative peak intensities remain also when $^{18}O_2$ is replaced with $^{16}O_2$ in sequence 3. At the lower temperature, 350 °C, it is likely that O_2 is less important for the formation of intermediate species and that the oxygen required mainly originates from NO_2.

4. Concluding Remarks

In the HC-SCR reaction, the hydrocarbon needs to be adsorbed and activated on the catalyst surface and the nitrogen oxide needs to be oxidized to NO_2. In this study, NO_2 is present already in the reaction gas mixture, and hence the adsorption and activation of the hydrocarbon is the crucial step. With DRIFT spectroscopy, formation of intermediate species can be followed during reaction conditions. When propane or isobutane is introduced to the sample cell, unsaturated hydrocarbons eventually form and simultaneously the Brønsted acid sites are blocked. Consequently, the Brønsted acid sites interact with the saturated hydrocarbons likely by donating a proton,[30] forming carbenium ion adsorbates and finally alkenes. In the presence of oxygen, the alkene formation proceeds faster. Introduction of NO_2 to the oxygen/propane mixture results in the formation of nitrosonium ions (NO^+), which likely react with the alkenes, forming isocyanate species, which, together with water formed in the reaction, can form amine species and finally N_2, via reaction with NO^+. Following the different functional groups on the sample surface during the reaction suggests that most of the reactions proceed over the Brønsted acid sites. However, when the propane acts as reducing agent, it will be oxidized, mainly to carbon dioxide. Experiments with isotope-labeled oxygen show an increased oxidation of propane with oxygen when NO_2 is present, as compared to when NO_2 is absent, in the reaction gas mixture, at the temperature where maximum NO_2 reduction occurs, that is, 450 °C. Hence, NO_2 facilitates the reaction between oxygen and propane, likely by initiating the oxidation of the propane-derived species (formed on the Brønsted acid sites) via a reaction mechanism where NO_2, either in the gas phase or loosely bound to the surface, reacts with carbenium ion adsorbates. The activated propane adsorbates may then further react with oxygen. At lower temperature (350 °C), NO_2 takes part in the oxidation of propane as well; however, at this temperature the promoting effect of NO_2 on the oxidation of propane with oxygen occurs only to a minor extent. The involvement of both oxygen and NO_2 in an effective oxidation of propane is also manifested by the detection of $NC^{18}O$ species adsorbed on the sample surface during reaction conditions. These species are observed in the temperature range that coincides with the maximum NO_2 reduction (450 °C), while at lower temperature no such species are identified. It is thus concluded that NO_2 plays a vital role in activating the propane for oxidation with oxygen under the conditions of this study.

Acknowledgment. We would like to thank Albemarle Catalysts BV for providing the zeolite. This work has been performed within the Competence Centre for Catalysis, which is hosted by Chalmers University of Technology and financially supported by the Swedish Energy Agency and the member companies: AB Volvo, Volvo Car Corporation, Scania CV AB, GM Powertrain Sweden AB, Haldor Topsøe A/S, Perstorp Specialty Chemicals AB, and The Swedish Space Agency.

References and Notes

(1) Iwamoto, M.; Yahiro, H.; Shundo, S.; Yu-u, Y.; Mizuno, N. *Shokubai (Catalyst)* **1990**, *32*, 430.
(2) Held, W.; Koenig, A.; Richter, T.; Puppe, L. *SEA Paper 900496*, 1990.
(3) Traa, Y.; Burger, B.; Weitkamp, J. *Microporous Mesoporous Mater.* **1999**, *30*, 3 and references therein.
(4) Parvulescu, V. I.; Grange, P.; Delmon, B. *Catal. Today* **1998**, *46*, 233 and references therein.
(5) Chen, H. Y.; Voskoboinikov, T.; Sachtler, W. M. H. *J. Catal.* **1999**, *186*, 91.
(6) Chen, H. Y.; Voskoboinikov, T.; Sachtler, W. M. H. *J. Catal.* **1998**, *180*, 171.
(7) Yeom, Y. H.; Wen, B.; Sachtler, W. M. H.; Weitz, E. *J. Phys. Chem. B* **2004**, *108*, 5386.
(8) Cowan, A. D.; Cant, N. W.; Haynes, B. S.; Nelson, P. F. *J. Catal.* **1998**, *176*, 329.
(9) Liu, I. O. Y.; Cant, N. W.; Haynes, B. S.; Nelson, P. F. *J. Catal.* **2001**, *203*, 487.
(10) Ingelsten, H. H.; Skoglundh, M. *Catal. Lett.* **2006**, *106*, 15.
(11) Ingelsten, H. H.; Zhao, D. M.; Palmqvist, A.; Skoglundh, M. *J. Catal.* **2005**, *232*, 68.
(12) Zhao, D. M.; Ingelsten, H. H.; Skoglundh, M.; Palmqvist, A. *J. Mol. Catal. A* **2006**, *249*, 13.
(13) Petunchi, J.; Hall, W. K. *Appl. Catal., B* **1993**, *2*, L17.
(14) Otsuka, K.; Takahashi, R.; Amakawa, K.; Yamanaka, I. *Catal. Today* **1998**, *45*, 23.
(15) Otsuka, K.; Takahashi, R.; Yamanaka, I. *J. Catal.* **1999**, *185*, 182.
(16) Lukyanov, D. B.; Sill, G.; d'Itri, J. L.; Hall, W. K. *J. Catal.* **1995**, *153*, 265.
(17) Hinz, A.; Skoglundh, M.; Fridell, E.; Andersson, A. *J. Catal.* **2001**, *201*, 247.
(18) Ingelsten, H. H.; Hildesson, Å.; Fridell, E.; Skoglundh, M. *J. Mol. Catal. A* **2004**, *209*, 199.
(19) Szostak, R. *Molecular Sieves*; Van Nostrand Reinhold: New York, 1989.
(20) Wallin, M.; Karlsson, C.-J.; Palmqvist, A.; Skoglundh, M. *Top. Catal.* **2004**, *30/31*, 107.
(21) Fanning, P. E.; Vannice, M. A. *J. Catal.* **2002**, *207*, 166.

(22) Chen, H. Y.; Voskoboinikov, T.; Sachtler, W. M. H. *Catal. Today* **1999**, *54*, 483.
(23) Xin, M.; Hwang, I. C.; Woo, S. I. *J. Phys. Chem. B* **1997**, *101*, 9005.
(24) Poignant, F.; Freysz, J. L.; Daturi, M.; Saussey, J. *Catal. Today* **2001**, *70*, 197.
(25) Hadjiivanov, K.; Saussey, J.; Freysz, J. L.; Lavalley, J. C. *Catal. Lett.* **1998**, *52*, 103.
(26) Szanyi, J.; Paffett, M. T. *J. Catal.* **1996**, *164*, 232.
(27) Trombetta, M.; Busca, G.; Rossini, S.; Piccoli, V.; Cornaro, U.; Guercio, A.; Catani, R.; Willey, R. J. *J. Catal.* **1998**, *179*, 581.
(28) Boskovic, G.; Vulic, T.; Kis, E.; Putanov, P. *Chem. Eng. Technol.* **2001**, *24*, 269.
(29) Mosqueda-Jimenez, B. I.; Jentys, A.; Seshan, K.; Lercher, J. A. *Appl. Catal., B* **2003**, *43*, 105.
(30) Jentoft, F. C.; Gates, B. C. *Top. Catal.* **1997**, *4*, 1.
(31) Hadjiivanov, K. I. *Catal. Rev.-Sci. Eng.* **2000**, *42*, 71.
(32) Beloshapkin, S. A.; Paukshtis, E. A.; Sadykov, V. A. *J. Mol. Catal. A* **2000**, *158*, 355.
(33) Obuchi, A.; Wogerbauer, C.; Koppel, R.; Baiker, A. *Appl. Catal., B* **1998**, *19*, 9.
(34) Yamaguchi, M. *J. Chem. Soc., Faraday Trans.* **1997**, *93*, 3581.
(35) Solymosi, F.; Bansagi, T. *J. Catal.* **1995**, *156*, 75.
(36) Park, S. K.; Choo, H.; Kevan, L. *Phys. Chem. Chem. Phys.* **2001**, *3*, 3247.
(37) Jobson, E.; Baiker, A.; Wokaun, A. *J. Chem. Soc., Faraday Trans.* **1990**, *86*, 1131.
(38) Topsoe, N. Y.; Topsoe, H.; Dumesic, J. A. *J. Catal.* **1995**, *151*, 226.
(39) Poignant, F.; Saussey, J.; Lavalley, J. C.; Mabilon, G. *Catal. Today* **1996**, *29*, 93.
(40) Park, S. K.; Park, Y. K.; Park, S. E.; Kevan, L. *Phys. Chem. Chem. Phys.* **2000**, *2*, 5500.
(41) Docquir, F.; Toufar, H.; Su, B. L. *Langmuir* **2001**, *17*, 6282.
(42) Su, B. L.; Norberg, V.; Hansenne, C. *Langmuir* **2000**, *16*, 1132.
(43) Acke, F.; Westerberg, B.; Skoglundh, M. *J. Catal.* **1998**, *179*, 528.
(44) Sun, Q.; Gao, Z. X.; Wen, B.; Sachtler, W. M. H. *Catal. Lett.* **2002**, *78*, 1.
(45) Svedberg, P.; Jobson, E.; Erkfeldt, S.; Andersson, B.; Larsson, M.; Skoglundh, M. *Top. Catal.* **2004**, *30*−*31*, 199.
(46) Ermini, V.; Finocchio, E.; Sechi, S.; Busca, G.; Rossini, S. *Appl. Catal., A* **2000**, *190*, 157.
(47) Olson, D. H.; Kokotailo, G. T.; Lawton, S. L.; Meier, W. M. *J. Phys. Chem.* **1981**, *85*, 2238.
(48) Liao, L. F.; Lien, C. F.; Shieh, D. L.; Chen, M. T.; Lin, J. L. *J. Phys. Chem. B* **2002**, *106*, 11240.
(49) Solymosi, F.; Bansagi, T.; Zakar, T. S. *Phys. Chem. Chem. Phys.* **2003**, *5*, 4724.
(50) Wichterlova, B.; Tvaruzkova, Z.; Sobalik, Z.; Sarv, P. *Microporous Mesoporous Mater.* **1998**, *24*, 223.